SAR COMPLIANCE TESTING OF CARD ACCESS MODEL MHI-CAWCB500 5.15 TO 5.35 GHz CARDBUS CARD INSERTED INTO A LAPTOP COMPUTER

July 18, 2001

Submitted to:

Mr. Nathan Mueller
Design Engineer
Card Access
71 North 490 West
American Fork, UT 84003

Submitted by:

Om P. Gandhi
Professor of Electrical Engineering
University of Utah
50 S Central Campus Dr., Rm. 3280
Salt Lake City, UT 84112-9206

SAR COMPLIANCE TESTING OF CARD ACCESS MODEL MHI-CAWCB500 5.15 TO 5.35 GHz CARDBUS CARD INSERTED INTO A LAPTOP COMPUTER

I. Introduction

The U.S. Federal Communications Commission (FCC) has adopted limits of human exposure to RF emissions from mobile and portable devices that are regulated by the FCC [1]. The FCC has also issued Supplement C (Edition 97-01) to OET Bulletin 65 [2] and a more recent version of the same [3] defining both the measurement and the computational procedures that should be followed for evaluating compliance of mobile and portable devices with FCC limits for human exposure to radiofrequency emissions.

We have used both the measurement and computational procedures for SAR compliance testing of the Card Access CardBus card (FCC ID: MHI-CAWCB500) inserted into a laptop computer. A photograph of the unit with the CardBus card inserted into the laptop computer is given in Fig. 1. A picture of the Model CAWCB500 CardBus card placed on the laptop is given in Fig. 2. For spatial diversity, the CardBus card uses two 5 GHz Side Stem Antennas each of geometry and dimensions given in Fig. 3. The antenna feed of width 1.75 mm and length 1.8 mm shown in Fig. 3 is mounted on a substrate of thickness 10 mils (0.25 mm) and dielectric constant 4.25. The two antennas are placed with a center-to-center spacing of 24.23 mm over a ground plane of width 43 mm and approximate length 45 mm. At any given time, only one of the two antennas is working either for the transmission or the reception mode. The Card Access Model CAWCB500 CardBus card operates with a transmit power to up to 16 dBm (40 mW).

Since the wireless PC may possibly be placed on a user's lap where the RF antennas would be the closest to the body, a planar phantom model was used both for SAR calculations as well as for SAR measurements.

II. Computation of SAR Distributions

The Finite Difference Time-Domain Method

One of the most successful and versatile methods for SAR calculations is the finite-difference time-domain (FDTD) method. This method was first proposed by Yee [4] and later developed by Taflove and colleagues [5-7], Holland [8], and Kunz and Lee [9]. This method has been extensively used for calculations of the distributions of electromagnetic (EM) fields and SARs in anatomically-based models of the human body for whole-body or partial-body exposures due to far-field or near-field irradiation conditions [10, 11]. In this method, the time-dependent Maxwell's curl equations

$$\nabla \times \mathbf{E} = -\mu \frac{\partial \mathbf{H}}{\partial t} \quad , \quad \nabla \times \mathbf{H} = \sigma \mathbf{E} + \varepsilon \frac{\partial \mathbf{E}}{\partial t} \tag{1}$$

are implemented for a lattice of sub volumes or "cells" that may be cubical or parallelepiped with different dimensions δ_x, δ_y, and δ_z in x-, y-, or z-directions, respectively. The components of **E** and **H** are positioned about each of the cells as shown in Fig. 4 and calculated alternately with half-time steps where the time step $\delta t = \delta/2c$ where δ is the smallest of the dimensions used for each of the cells and c is the maximum phase velocity of the fields in the modeled space. Since some of the modeled volume is air, c corresponds to the velocity of EM waves in air. The details of the method are given in several of the above referenced publications [4-9] and will, therefore, not be repeated here.

In the FDTD method, it is necessary to represent not only the scatterer/absorber such as the human body or a part thereof, but also any near-field sources/s such as the Side Stem Antenna of Fig. 3 mounted into a laptop computer. Since the SAR distribution is critically dependent on the antenna geometry and its placement vis à vis the lossy planar model simulant of the human lap, this region was modeled with an FDTD cell size of $0.6 \times 0.6 \times 0.6$ mm. This choice of the cell dimensions allowed a proper

representation of the stem antenna height (3.6 mm), its width (1.75 or nearly 1.8 mm), the top loading circular hat (diameter 8.4 mm) and the antenna feed of width 1.75 or 1.8 mm and length 1.8 mm), the ground plane of dimensions (42 × 74.4 mm) and the separation between the bottom of the ground plane to the top of the lap-simulant model of 1.08 cm (18 cells). For SAR calculations, we have assumed a planar muscle-simulant lossy phantom at a distance of 1.08 cm below the CardBus card ground plane to account for a part of the thickness of the PC keyboard. For this planar model of dimensions 13.8 × 10.8 × 5.4 cm modeled by 230 × 180 × 90 cells (of dimension 0.6 mm), we have used muscle-simulant dielectric properties of ε_r = 49.22 and conductivity σ = 4.32 S/m taken from the FCC website [www.fcc.gov/fcc-bin/dielec.sh]. Similar to the FDTD cell size used for modeling of the antenna, this planar tissue-simulant is also modeled by a cell size of 0.6 mm. A graphical representation of the SAR distributions calculated for the surface layer and for three additional layers at depths of 3, 6, and 9 mm are shown in Fig. 5, respectively. For all of these calculations, the antenna excited for a total radiated power of 16 dBm (40 mW) is assumed to be in the upper right hand corner which explains the high SARs for the phantom underneath. The calculated power absorbed by the entire phantom is 8.20 mW (20.5% of the conducted power) and the peak 1-g SAR is 0.176 W/kg.

For SAR calculations, we have also used a second tissue-simulant phantom which is a proper representation of the rectangular box phantom used for experimental SAR measurements (see Fig. 7). This box phantom described in detail in Section V uses an acrylic base of thickness 6.35 mm and dielectric constant ε_r = 2.56. For the present calculations, we have represented this base by 10 layers of FDTD cells thus increasing the distance to the first muscle-simulant lossy layer from 10.8 to 16.8 mm. The SAR distributions calculated for this phantom are given in Fig. 6 for the top lossy layer and at depths of 3, 6, and 9 mm, respectively. As expected, the peak 1-g SAR of 0.129 W/kg is

somewhat lower. Also the calculated power absorbed by the phantom is 6.24 mW which is lower than 8.20 mW for the phantom in contact with the base of the laptop.

III. Effect of the Size of the Ground Plane on SAR Distributions

The highest SARs are expected for the lossy planar phantom for the region underneath the Side Stem Antenna sketched in Fig. 3. This is indeed true for the FDTD-calculated SAR distributions sketched in Figs. 5 and 6, respectively. Also as expected, the SARs drop off very rapidly at 5.25 GHz and are increasingly lower at depths of 3, 6, and 9 mm, respectively both for a muscle-simulant phantom at a spacing of 1.08 cm below the CardBus card ground plane (in contact with the base of the laptop) or with a top acrylic lid of 6 mm to simulate the phantom used for experimental measurements. For both of these cases, the peak 1-g SARs are not likely to be impacted much by the physical extent of the ground plane or by the laptop computer. This is validated by calculating the peak 1-g SAR for CardBus card ground plane dimensions of 42.6×44.4 mm (71×74 cells) or 42.6×74.4 mm (71×124 cells). The peak 1-g SARs calculated for the phantom with 6 mm top acrylic lid are 0.126 and 0.129 W/kg for the two cases, respectively. A difference of just 0.003 W/kg confirms that, as expected, the highest internal tissue fields occur for the region beneath the antenna and the effect of length of the ground plane on the SAR distributions is relatively insignificant.

IV. Calculations of the Antenna Pattern in Free Space

The FDTD method may be used to calculate the radiation pattern of the Card Access Model CAWCB500 CardBus card inserted into a laptop computer in free space so that it may be compared with the data available from the manufacturer. Since most of the microwave-induced currents for the antenna are for the ground plane immediately underneath the Side Stem Antenna, only a limited length of the ground plane beyond the antenna should be enough for proper modeling of the radiated fields. This is verified by

calculating the gain of the CardBus card antenna for ground plane dimensions of 42.6 × 44.4 mm (71 × 74 cells) or 42.6 × 74.4 mm (71 × 124 cells). The calculated gains are 3.70 and 3.59 dBi, respectively. Both of these values are very close to the manufacturer measured gain of 3.9 dBi for this antenna.

V. Experimental Measurements of SAR Distribution

The testing of the SAR distribution for the Card Access Model CAWCB500 CardBus card inserted into a laptop computer was done with a planar rectangular box phantom shown in Fig. 7. This box phantom of external dimensions 30 × 50 cm is filled with a tissue-simulant fluid up to a depth of 15.5 cm. To maintain flatness of the phantom, the rectangular box is made of acrylic (ε_r = 2.56) of thickness 6.35 mm. The tissue-simulant fluid uses a composition developed at the University of Utah which consists of 61.0% water, 38.0% sugar and 1% HEC. For this composition, we have measured the dielectric properties using a Hewlett Packard (HP) Model 85070B Dielectric Probe in conjunction with HP Model 8720C Network Analyzer (50 MHz-20 GHz). The measured dielectric properties at the mid band frequency of 5.25 GHz are as follows: $\varepsilon_r = 48.5 \pm 1.7$ and $\sigma = 4.28 \pm 0.08$ S/m. From the FCC website, we obtain the desired dielectric properties to simulate the muscle tissue to be $\varepsilon_r = 49.22$ and $\sigma = 4.32$ S/m. Thus, the measured properties for the muscle-simulant fluid are close to the desired values.

VI. Calibration of the E-Field Probe

As in some previously reported SAR measurements at 6 GHz [12], we have calibrated the Narda Model 8021 Miniature Broadband Electric Field Probe (0.4 to 10 GHz) using a rectangular waveguide WR 159 that was filled with this muscle-simulant fluid at 5.25 GHz. By comparing the electric fields expected in the tissue from the analytical expressions of the waveguide theory, we obtain a calibration factor of 2.98

(mW/kg)/μV. This is considerably larger than calibration factors of 0.39 and 0.565 (mW/kg)/μV previously reported for the same probe at 835 MHz and 1900 MHz, respectively. This is to be expected since the sensitivity of the diodes used for the Narda Model 8021 Miniature Broadband Electric Field Probe is likely to diminish with frequency.

VII. The Measured SAR Distributions

The SAR distribution was determined using the automated SAR measurement system developed at the University of Utah [13]. As described in [13], this SAR measurement system has been validated using a number of wireless telephones at 835 and 1900 MHz, respectively.

The highest SAR region for each of the channels was identified in the first instance by using a coarser sampling with a step size of 8.0 mm over three overlapping areas for a total scan area of 8.0 × 9.6 cm. After identifying the region of the highest SAR, the SAR distribution was measured with a resolution of 2 mm in order to obtain the peak 1 cm^3 or 1-g SAR.

The SAR distributions were measured and are given in Tables 1-3 at a low end, midband and high end frequencies of 5.18, 5.25, and 5.32 GHz, respectively. The peak 1-g SARs thus obtained are summarized in Table 4 and vary from 0.102-0.134 W/kg. The measured peak 1-g SARs are extremely close to those calculated for the Model CAWCB500 CardBus card antenna (see Sections II, III).

VIII. Comparison of the Data With FCC 96-326 Guidelines

According to the FCC 96-326 Guidelines [1], the peak SAR for any 1-g of tissue should not exceed 1.6 W/kg. For the maximum radiated power condition of 16 dBm (40 mW), the Card Access Model CAWCB500 CardBus card has been measured to give peak 1-g SARs of 0.102-0.134 W/kg which are considerably smaller than 1.6 W/kg.

REFERENCES

1. Federal Communications Commission, "Guidelines for Evaluating the Environmental Effects of Radiofrequency Radiation," FCC 96-326, August 1, 1996.

2. K. Chan, R. F. Cleveland, Jr., and D. L. Means, "Evaluating Compliance With FCC Guidelines for Human Exposure to Radiofrequency Electromagnetic Fields," Supplement C (Edition 97-01) to OET Bulletin 65, December, 1997. Available from Office of Engineering and Technology, Federal Communications Commission, Washington D.C., 20554.

3. Federal Communications Commission "Supplement C Edition 01-01 to OET Bulletin 65 Edition 97-01" June 2001.

4. K. S. Yee, "Numerical Solution of Initial Boundary Value Problems Involving Maxwell's Equations in Isotropic Media," *IEEE Transactions on Antennas and Propagation,* Vol. AP-14, pp. 302-307, 1966.

5. A. Taflove and M. E. Brodwin, "Computation of the Electromagnetic Fields and Induced Temperature Within a Model of the Microwave Irradiated Human Eye," *IEEE Transactions on Microwave Theory and Techniques,* Vol. MTT-23, pp. 888-896, 1975.

6. A. Taflove, "Application of the Finite-Difference Time-Domain Method to Sinusoidal Steady-State Electromagnetic-Penetration Problems," *IEEE Transactions on Electromagnetic Compatibility,* Vol. EMC-22, pp. 191-202, 1980.

7. K. Umashankar and A. Taflove, "A Novel Method to Analyze Electromagnetic Scattering of Complex Objects," *IEEE Transactions on Electromagnetic Compatibility,* Vol. EMC-24, pp. 397-405, 1982.

8. R. Holland, "THREDE: A Free-Field EMP Coupling and Scattering Code," *IEEE Transactions on Nuclear Science,* Vol. NS-24, pp. 2416-2421, 1977.

9. K. S. Kunz and K. M. Lee, "A Three-Dimensional Finite-Difference Solution of the External Response of an Aircraft to a Complex Transient EM Environment. The Method and Its Implementation," *IEEE Transactions on Electromagnetic Compatibility,* Vol. 20, pp. 328-3342, 1978.

10. O. P. Gandhi, "Some Numerical Methods for EM Dosimetry: ELF to Microwave Frequencies," *Radio Science,* Vol. 30, pp. 161-177, January/February, 1995.

11. O. P. Gandhi, G. Lazzi, and C. M. Furse, "Electromagnetic Absorption in the Human Head and Neck for Mobile Telephones at 835 and 1900 MHz," *IEEE Transactions on Microwave Theory and Techniques,* Vol. 44(10), pp. 1884-1897, 1996.

12. O. P. Gandhi and J-Y. Chen, "Electromagnetic Absorption in the Human Head from Experimental 6-GHz Handheld Transceivers," *IEEE Transactions on Electromagnetic Compatibility*, Vol. 39(4), pp. 547-558, 1995.

13. Q. Yu, O. P. Gandhi, M. Aronsson, and D. Wu, "An Automated SAR Measurement System for Compliance Testing of Personal Wireless Devices," *IEEE Transactions on Electromagnetic Compatibility*, Vol. 41(3), pp. 234-245, August 1999.

Table 1. The SARs measured for the Card Access Model CAWCB500 CardBus card inserted into a laptop computer for the **low end frequency of 5.18 GHz.** The SARs in W/kg are measured with a step size of 2 mm for the highest SAR region.

1-g SAR = 0.124 W/kg

a. At depth of 1 mm

0.159	0.194	0.207	0.174	0.221
0.208	0.195	0.213	0.190	0.229
0.197	0.225	0.223	0.212	0.217
0.197	0.236	0.210	0.236	0.213
0.205	0.225	0.188	0.213	0.222

b. At depth of 3 mm

0.123	0.148	0.152	0.134	0.155
0.155	0.151	0.161	0.147	0.173
0.154	0.167	0.165	0.164	0.163
0.152	0.167	0.168	0.183	0.157
0.143	0.163	0.157	0.163	0.155

c. At depth of 5 mm

0.093	0.111	0.107	0.099	0.103
0.112	0.115	0.119	0.111	0.128
0.119	0.120	0.118	0.125	0.119
0.114	0.114	0.133	0.138	0.110
0.095	0.115	0.129	0.122	0.102

d. At depth of 7 mm

0.069	0.082	0.071	0.072	0.067
0.078	0.086	0.086	0.081	0.093
0.091	0.086	0.083	0.094	0.084
0.085	0.076	0.104	0.102	0.074
0.060	0.080	0.103	0.089	0.062

e. At depth of 9 mm

0.049	0.062	0.045	0.051	0.046
0.055	0.065	0.061	0.059	0.068
0.071	0.064	0.060	0.071	0.059
0.065	0.052	0.083	0.074	0.047
0.039	0.059	0.079	0.066	0.035

Table 2. The SARs measured for the Card Access Model CAWCB500 CardBus card inserted into a laptop computer for the **midband frequency of 5.25 GHz.** The SARs in W/kg are measured with a step size of 2 mm for the highest SAR region.

1-g SAR = 0.134 W/kg

a. At depth of 1 mm

0.197	0.202	0.201	0.205	0.202
0.200	0.207	0.226	0.195	0.194
0.196	0.220	0.213	0.211	0.237
0.182	0.204	0.212	0.236	0.222
0.228	0.200	0.228	0.251	0.220

b. At depth of 3 mm

0.146	0.153	0.150	0.158	0.153
0.157	0.153	0.168	0.151	0.150
0.154	0.165	0.163	0.163	0.178
0.140	0.161	0.166	0.178	0.177
0.176	0.163	0.182	0.200	0.187

c. At depth of 5 mm

0.106	0.113	0.109	0.120	0.113
0.120	0.111	0.122	0.115	0.114
0.119	0.121	0.122	0.125	0.130
0.107	0.126	0.129	0.132	0.140
0.133	0.132	0.146	0.158	0.160

d. At depth of 7 mm

0.077	0.081	0.078	0.090	0.081
0.092	0.081	0.086	0.086	0.086
0.090	0.088	0.089	0.097	0.095
0.083	0.099	0.100	0.100	0.111
0.102	0.107	0.119	0.127	0.139

e. At depth of 9 mm

0.060	0.057	0.058	0.069	0.059
0.071	0.063	0.063	0.063	0.066
0.069	0.066	0.066	0.078	0.072
0.068	0.081	0.080	0.080	0.090
0.081	0.090	0.101	0.105	0.122

Table 3. The SARs measured for the Card Access Model CAWCB500 CardBus card inserted into a laptop computer for the **high end frequency of 5.32 GHz.** The SARs in W/kg are measured with a step size of 2 mm for the highest SAR region.

1-g SAR = 0.102 W/kg

a. At depth of 1 mm

0.167	0.165	0.135	0.142	0.169
0.148	0.194	0.115	0.168	0.146
0.151	0.153	0.153	0.138	0.155
0.151	0.154	0.151	0.185	0.181
0.185	0.173	0.159	0.173	0.173

b. At depth of 3 mm

0.132	0.121	0.109	0.117	0.127
0.118	0.144	0.106	0.127	0.119
0.109	0.121	0.118	0.108	0.117
0.128	0.126	0.128	0.133	0.134
0.137	0.137	0.122	0.139	0.133

c. At depth of 5 mm

0.102	0.087	0.087	0.095	0.094
0.093	0.104	0.095	0.094	0.096
0.076	0.092	0.088	0.083	0.088
0.107	0.101	0.107	0.093	0.097
0.099	0.106	0.092	0.111	0.100

d. At depth of 7 mm

0.077	0.063	0.070	0.076	0.070
0.073	0.074	0.083	0.069	0.077
0.052	0.069	0.063	0.064	0.065
0.088	0.079	0.089	0.066	0.069
0.070	0.080	0.069	0.089	0.074

e. At depth of 9 mm

0.057	0.049	0.057	0.060	0.053
0.059	0.053	0.069	0.051	0.062
0.038	0.050	0.041	0.050	0.050
0.070	0.060	0.072	0.051	0.050
0.052	0.059	0.052	0.071	0.054

Table 4. Summary of the measured peak 1-g SAR for the Card Access Model CAWCB500 CardBus card inserted into a laptop computer for the maximum radiated power of 16 dBm (40 mW).

Frequency GHz	1-g SAR (W/kg)
5.18	0.124
5.25	0.134
5.32	0.102

Fig. 1. Photograph of the Card Access Model CAWCB500 CardBus card inserted into a laptop computer.

Fig. 2. A picture of the Model CAWCB500 CardBus card placed on the laptop computer.

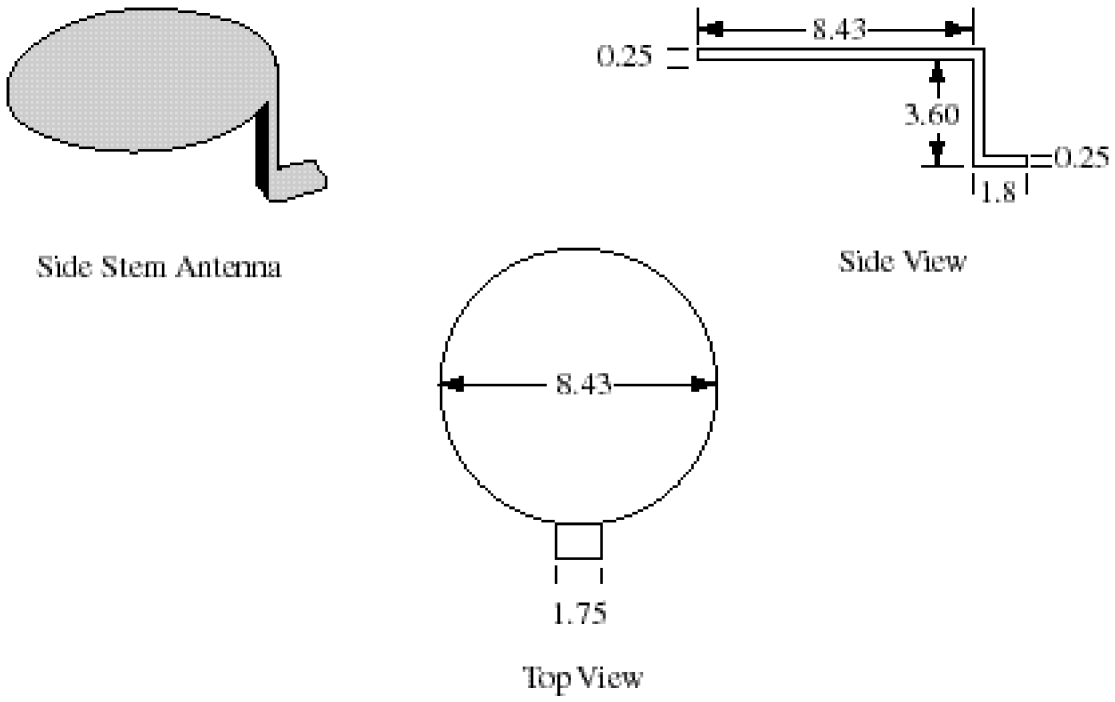

Fig. 3. A 5 GHz Side Stem Antenna and its dimensions (all dimensions in mm).

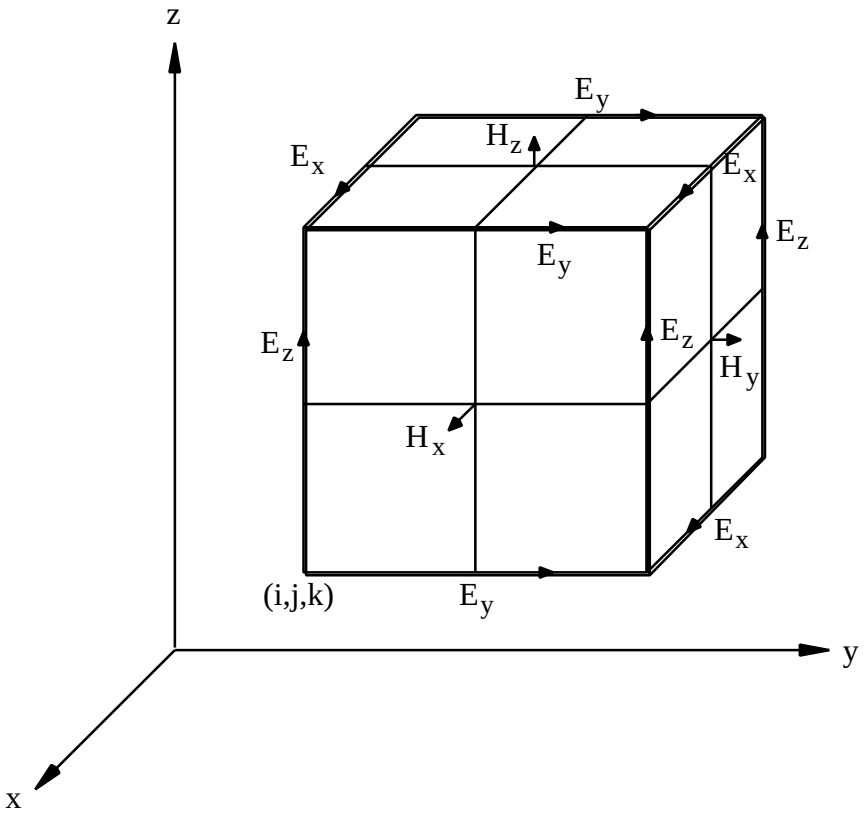

Fig. 4. A unit cell of Yee lattice indicating positions for the various field components.

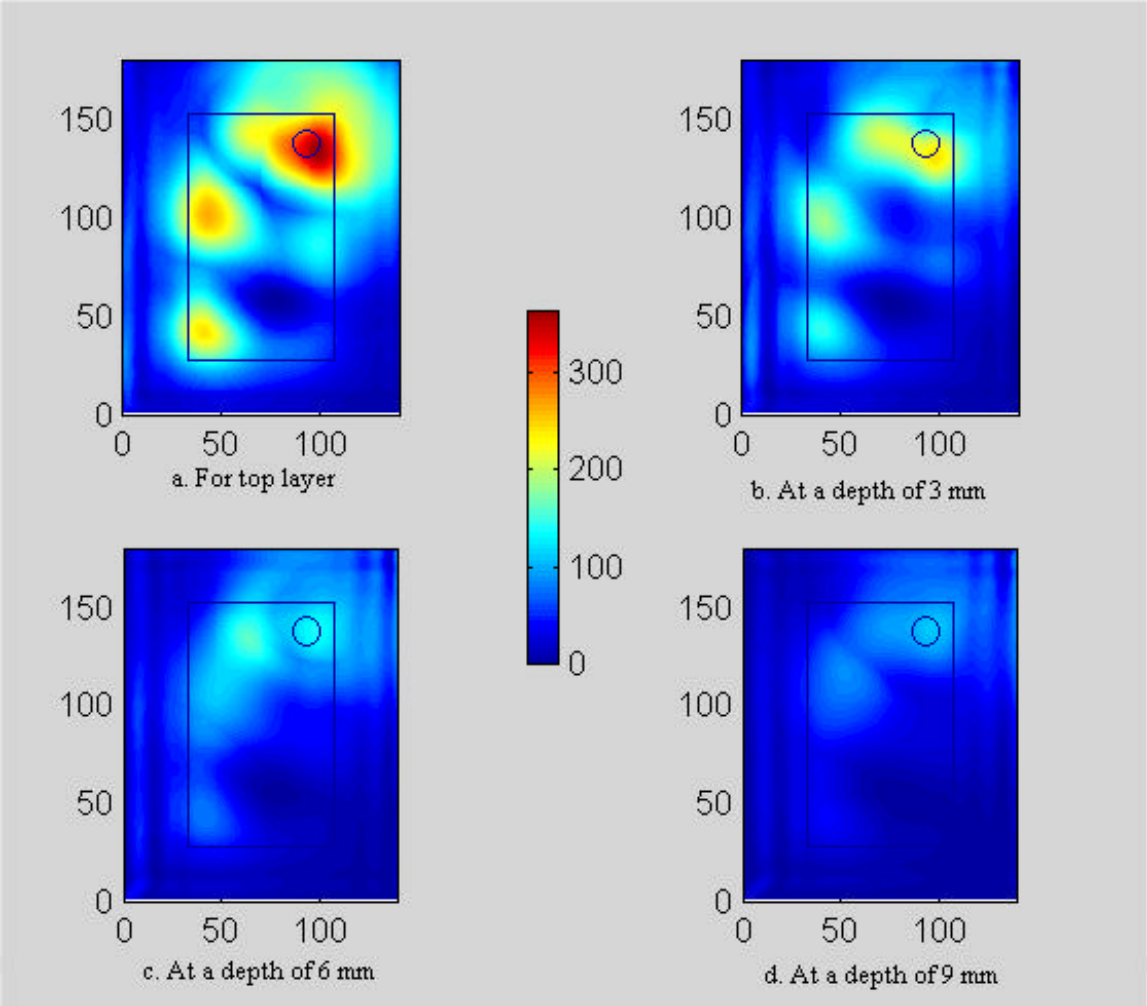

Fig. 5. The calculated SAR distributions at 5.25 GHz for the Card Access Model CAWCB500 CardBus card for a planar muscle-simulant phantom in contact with the bottom surface of the laptop computer. Peak 1-g SAR = 0.176 W/kg.

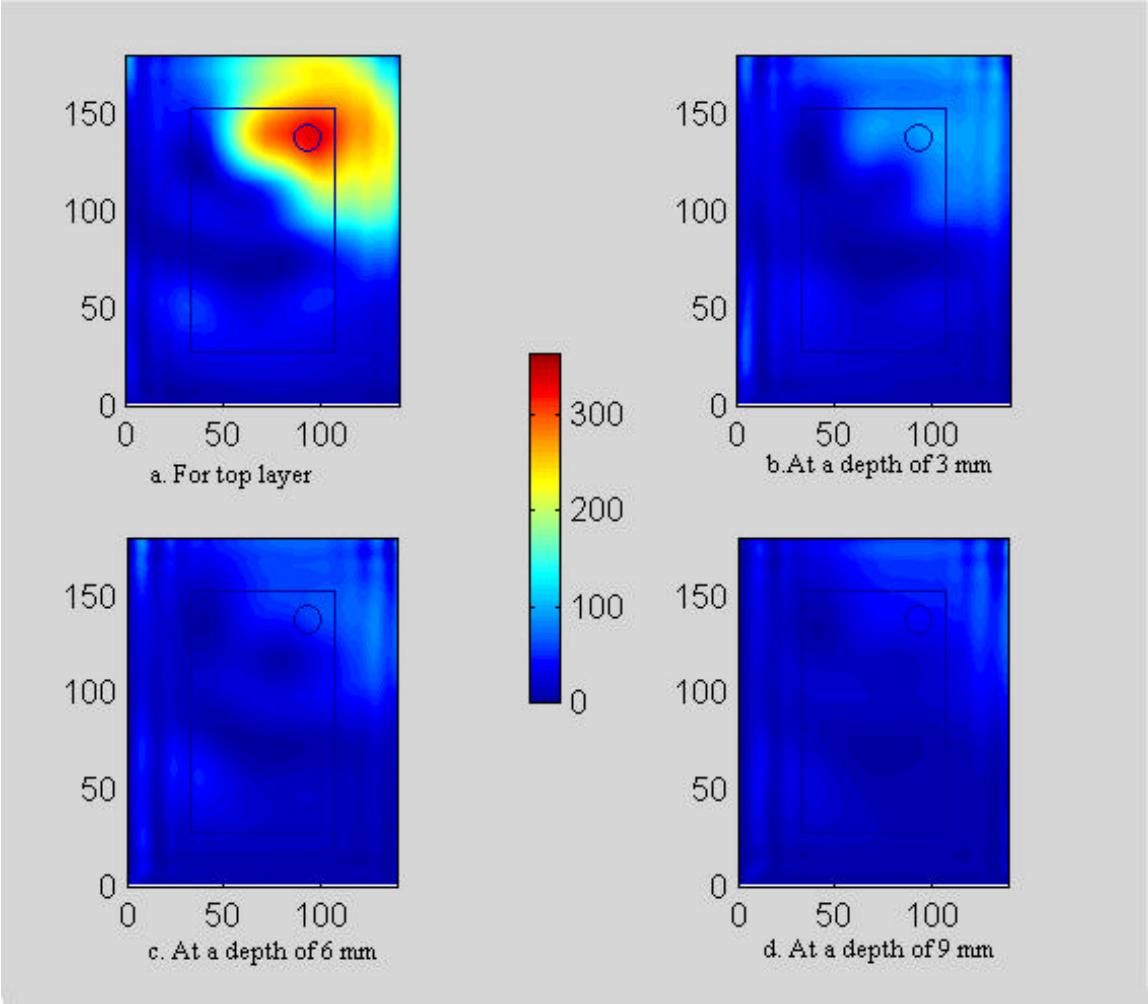

Fig. 6. The calculated SAR distributions at 5.25 GHz for the Card Access Model CAWCB500 CardBus card for a planar muscle-simulant model covered by an acrylic (ε_r = 2.56) box of thickness 6 mm. Peak 1-g SAR = 0.129 W/kg.

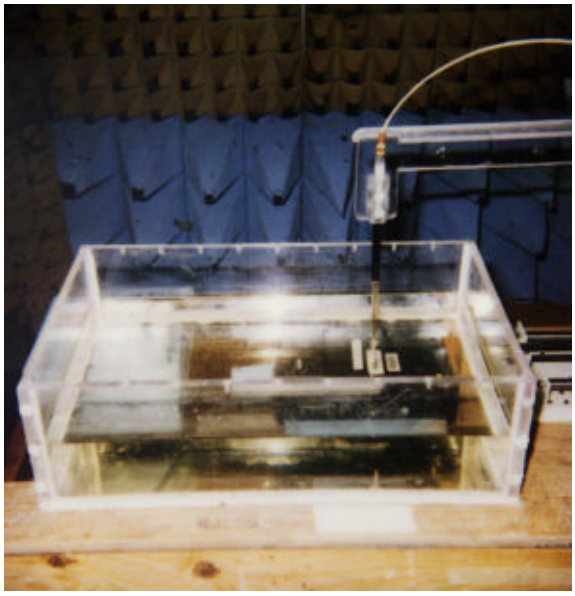

Fig. 7. Photograph of the Card Access Model CAWCB500 CardBus card inserted into a laptop computer with its bottom pressed against the bottom of the planar tissue-simulant phantom.